JCTC Journal of Chemical Theory and Computation

Article

pubs.acs.org/JCTC

Harmonic Models in Cartesian and Internal Coordinates to Simulate the Absorption Spectra of Carotenoids at Finite Temperatures

Javier Cerezo,* José Zúñiga, and Alberto Requena

Departamento de Química Física, Universidad de Murcia, 30100 Murcia, Spain

Francisco J. Ávila Ferrer

CNR−Consiglio Nazionale delle Ricerche, Istituto di Chimica dei Composti Organometallici (ICCOM-CNR), UOS di Pisa, Area della Ricerca, via G. Moruzzi 1, I-56124 Pisa, Italy and

Physical Chemistry, Faculty of Science, University of Málaga, Málaga 29071, Spain

Fabrizio Santoro*

CNR−Consiglio Nazionale delle Ricerche, Istituto di Chimica dei Composti Organo Metallici (ICCOM-CNR), UOS di Pisa, Area della Ricerca, via G. Moruzzi 1, I-56124 Pisa, Italy

Supporting Information

ABSTRACT: When large structural displacements take place between the ground state (GS) and excited state (ES) minima of polyatomic molecules, the choice of a proper set of coordinates can be crucial for a reliable simulation of the vibrationally resolved absorption spectrum. In this work, we study two carotenoids that undergo structural displacements from GS to ES minima of different magnitude, from small displacements for violaxanthin to rather large ones for β-carotene isomers. Their finite-temperature (77 and 300 K) spectra are simulated at the harmonic level, including Duschinsky effect, by time-dependent (TD) and time-independent (TI) approaches, using (TD)DFT computed potential energy surfaces (PES). We adopted two approaches to construct the harmonic PES, the Adiabatic (AH) and Vertical Hessian (VH) models and, for AH, two reference coordinate frames: Cartesian and valence internal coordinates. Our results show that when large displacements take place, Cartesian coordinates dramatically fail to describe curvilinear displacements and to account for the Duschinsky matrix, preventing a realistic simulation of the spectra within the AH model, where the GS and ES PESs are quadratically expanded around their own equilibrium geometry. In contrast, internal coordinates largely amend such deficiencies and deliver reasonable spectral widths. As expected, both coordinate frames give similar results when small displacements occur. The good agreement between VH and experimental line shapes indicates that VH model, in which GS and ES normal modes are both evaluated at the GS equilibrium geometry, is a good alternative to deal with systems exhibiting large displacements. The use of this model can be, however, problematic when imaginary frequencies arise. The extent of the nonorthogonality of the Dushinsky matrix in internal coordinates and its correlation with the magnitude of the displacement of the GS and ES geometries is analyzed in detail.

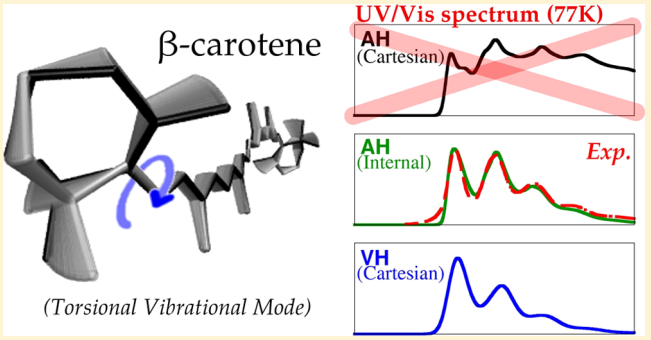

1. INTRODUCTION

Computational spectroscopy has emerged as a powerful tool to interpret and complement experimental spectroscopic data, and it aims to simulate, from first principles, spectra directly comparable with the experiment. Both time-independent (TI) and time-dependent (TD) approaches are available to compute vibrationally resolved electronic spectra (see refs 1−4 for recent reviews). The main challenges for the accurate simulation of the spectra are represented by the need for reliable descriptions of the ground state (GS) and excited state (ES) energies and the proper account of the solvent effects and the possible anharmonicities of the GS and ES potential energy surface (PES). While theoretical tools to properly face each of the aforementioned issues do exist, such as highly correlated electronic structure methods, implicit solvent models,[5] and anharmonic treatments,[6,7] they may become impractical when dealing with large systems. As a consequence, quadratic

Received: July 4, 2013

dx.doi.org/10.1021/ct4005849 | J. Chem. Theory Comput. XXXX, XXX, XXX−XXX

(harmonic) expansions of the PES around some reference geometries still represent, at the state-of-the-art, a necessary approximation for full-dimensionality treatments of such systems, and when needed, they also provide the suitable framework to separate some modes and treat them anharmonically in subsequent refinements. Even within the harmonic approach, however, some additional problems arise, associated to the limitations of representing the normal modes in terms of standard coordinate frames. Indeed, linear Cartesian coordinates are not adequate to describe large displacements of curvilinear modes, such as torsions, as they involve artificial bond stretching along the curvilinear displacement.[8] Consequently, more suitable coordinate frames are desirable to describe curvilinear motions. Valence internal coordinates, such as bond lengths, angles and dihedral angles were adopted in the seminal article of Sharp and Rosenstock on the calculation of Franck−Condon (FC) factors in polyatomic molecules.[9] More recently, in 2001, Reimers proposed a practical method to compute the Duschinsky matrix in internal coordinates,[8] and Borrelli et al. first documented the inadequacy of a representation in Cartesian coordinates for the simulation of the electronic spectrum of a prototype system exhibiting large displacements (i.e., ethylene in the $N \rightarrow V$ transition), showing that the usage of internal coordinates provided much better results.[10] The same authors adopted internal coordinates to simulate spectra of a number of small- and medium-size flexible molecules.[4,11,12]

Computation of the electronic spectra is usually based on the use of the first-order Duschinsky transformation,[13] which connects the GS and ES normal modes through a rotation matrix and a displacement vector. The evaluation of these quantities certainly depend on the model adopted to construct the harmonic PES and on the coordinate frame used to describe the normal modes. Harmonic models for the PES differ for the nuclear geometry from which the ES Hessian information is retrieved, which can be either the ES[9] or the GS[14] minimum, and we recently proposed to name these two models Adiabatic Hessian (AH) and Vertical Hessian (VH),[1,15] respectively (Nooijen and co-workers use the terms adiabatic Franck−Condon and Vertical Franck−Condon[16]). Vertical and adiabatic approaches have been compared in a number of contributions, already in the early stage of this research field[17] and in more recent papers (see, for example, refs [18−20]). An extensive comparison of AH and VH models, and of the set of simplified models that can be derived from them neglecting either off-diagonal or all the quadratic couplings, is given in ref 15 for rigid systems. In the AH model, GS and ES normal modes are defined at different geometries and the accurate description of the displaced normal modes becomes crucial; the use of either Cartesian or internal coordinates may lead then to very different results.

Aiming at investigating the performance of different harmonic models to simulate the electronic spectra of medium-large systems, we have focused on two carotenoids: β-carotene and violaxanthin (Figure 1). Despite their structural similarities, the conformational deviations from GS to ES in these two molecules are significantly different, thus allowing a systematic comparison of all different models as a function of such structural displacement; this offers quite a complete view of their strengths and weaknesses. Furthermore, carotenoids are important natural pigments,[21,22] and the details of their photoexcited dynamics, involving several electronic states, are still a matter of debate.[23] In this context, the development of

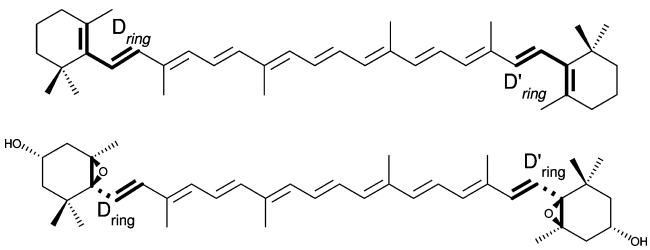

Figure 1. Molecular structure of β-carotene (top) and violaxanthin (bottom). The torsion angles connecting the ionone ring with the conjugated chain (D_{ring} and D'_{ring}) are highlighted on the structures.

efficient methods to reliably simulate their electronic spectra becomes very important. In this work, we focus on the simulation of the most intense spectroscopic band of these carotenoids, which corresponds to the transition between the $1^1A_g^-$ (S_0) and the $1^1B_{1u}^+$ (S_2) states, at finite temperature. It is worth noticing that Götze and Thiel[24] have recently simulated this band in violaxanthin and zeaxanthin at 0 K using the AH model with the normal modes described in Cartesian coordinates, evidencing some important problems in the case of zeaxanthin; in the following, we show that these problems arise from a partial failure of the AH model to describe the Duschinsky transformation.

Experimentally, the number of spectroscopic studies of carotenoids has increased steeply in the last decades, and nowadays, the electronic spectrum of many carotenoids is available at both cryogenic and room temperatures.[22] The bright $S_0 \rightarrow S_2$ transition is normally characterized by pretty well resolved vibronic spectrum at low temperatures, showing progression bands which are assigned to C═C and C−C stretching modes,[25] with the first (0−0) band usually carrying the strongest intensity. At higher temperatures, however, the shape of the spectrum noticeably changes showing a large broadening and, in some cases, a shift of the most intense vibronic feature from the first band (0−0) at low temperatures to the second one (0−1) at room temperature. These effects are observed in several carotenoids, including carotenes and xanthophylls with ring-closed and opened chain endings.[26−31] Interestingly, the vast amount of spectroscopic information available in this respect constitutes a valuable reference to benchmark the electronic calculations and theoretical approaches to simulate the spectra.

On the computational side, one of the main challenges at simulating the electronic spectra of carotenoids is the multireference nature of some of the excited states of carotenoids such as $2^1A_g^-$ (S_1), $1^1B_{1u}^-$ and $3^1A_g^-$, which have important contributions from double excitations as reported for series of polyenes[32] and carotenoids.[33] Nevertheless, the states involved in the one-photon allowed transition considered in this work, that is, $1^1A_g^-$ (S_0) and $1^1B_{1u}^+$ (S_2), can be adequately described using Density Functional Theory (DFT) (S_0) and the monoreferencial single excitation method Time Dependent (TD) DFT method (S_2). Comparisons with the experimental spectra are expected to give further insights on the accuracy of the DFT computed potential energy surface (PES) for these molecules.

The paper is organized as follows: Section 2 briefly reviews the theoretical models proposed to simulate of the vibronic spectra of carotenoids, including the adiabatic and vertical models and the use of internal coordinates. Section 3 describes the computational methods employed to carry out the

dx.doi.org/10.1021/ct4005849 | J. Chem. Theory Comput. XXXX, XXX, XXX−XXX

electronic calculations and subsequently compute the spectra within TD and TI formalisms. The results obtained in the simulations of the spectra of the two carotenoids are presented in Section 4. Section 5 contains the conclusions.

2. THEORETICAL MODELS

In the TI approach, the simulation of vibrationally resolved electronic absorption spectra is carried out through the sum over all individual transitions from every vibrational state ($|v'\rangle$, with energy $\hbar\omega_{v'}$) in the initial electronic state ($|e'\rangle$), weighted by their Boltzmann populations, to the vibrational levels ($|v\rangle$, with energy $\hbar\omega_v$) of the final electronic state ($|e\rangle$).[1] The expression for the spectrum intensity as function of the frequency, $S(\omega)$, can therefore be written as

$$S(\omega) = C\omega \sum_{v,v'} \rho_{v'}(T)|\langle \mathbf{v}'|\mu_{e',e}|\mathbf{v}\rangle|^2 \delta(\omega_v + \Delta E - \omega_{v'} - \omega) \tag{1}$$

where C is a constant whose actual derivation can be found in the literature (e.g., in ref 1), $\rho_{v'}$ is the Boltzmann population of the vibrational state $\mathbf{v}'$, ΔE the adiabatic energy difference between the minima of the ES and GS PESs, and $\mu_{e',e}$ is the electronic transition dipole moment.

The above expression can be reformulated in the time domain (i.e., within a TD approach), as the Fourier transform of the finite-temperature time correlation function, $\chi(t,T)$[2,34] as follows

$$S(\omega) = \frac{C\omega}{2\pi Z_v} \int \chi(t, T) e^{-it(\Delta E/\hbar - \omega)} dt \tag{2}$$

where Z_v is the vibrational partition function. The time correlation function is provided by

$$\chi(t, T) = \mathrm{Tr}[\mu_{e',e} e^{-itH_e/\hbar} \mu_{e',e} e^{-(\beta - it/\hbar)H_g}] \tag{3}$$

where Tr refers to the trace operation, β is the inverse of the product of the Boltzmann factor by the temperature, and H_g and H_e are the ground-state and excited-state Hamiltonians, respectively.

We adopt harmonic approximation to describe the GS and ES PESs and consider the linear Duschinsky relation[13] between the GS and ES normal modes:

$$\mathbf{Q}_g = \mathbf{J}\mathbf{Q}_e + \mathbf{K} \tag{4}$$

where $\mathbf{Q}_g$ and $\mathbf{Q}_e$ are the normal mode coordinates of the ground and excited states, $\mathbf{J}$ is the Duschinsky matrix and $\mathbf{K}$ is the displacement vector.

The GS harmonic PES is built by a quadratic expansion around its minimum, that is, computing the Hessian matrix at this geometry. AH and VH models are used for the ES PES.[15] Within the AH model, the ES harmonic potential is reconstructed at the ES minimum; whereas within the VH model, the harmonic potential is generated at the GS minimum (Franck–Condon point), from the ES energy, gradient, and Hessian. The AH model has the advantage that the Hessian is computed at a minimum and only real vibrational frequencies therefore appear. The VH model may, on the contrary, feature some imaginary frequencies whose treatment should, in principle, go beyond the harmonic approximation. On the other hand, as we will show below, the use of VH model is beneficial when large displacement from the ground- to excited-state minima occur for two reasons. First, the region of the ES PES, which is more relevant for the spectrum shape is the one spanned by the GS vibrational wave functions thermally populated, that is, the Franck–Condon (FC) region,[16] and second, GS and ES normal modes are defined at the same point, and therefore, their Duschinsky relation does not suffer from the issues of Cartesian coordinates to describe curvilinear displacements discussed below.

As far as the transition dipole moment $\mu_{e',e}$ is concerned, the $S_0 \rightarrow S_2$ transitions of carotenoids are bright and it is possible to invoke the Condon approximation (i.e., $\mu_{e',e} = \mu^0_{e',e}$), where $\mu^0_{e',e}$ is the value computed at the GS structure.

Different effective strategies have been proposed to compute the spectra with both TI[35−38] and TD[34,39,40] methods, adopting Cartesian coordinates. In some cases, however, such as when large normal mode displacements occur between GS and ES minima, other coordinate frames, especially valence internal coordinates, might be more appropriate to describe the curvilinear motion along normal modes.[8,10−12]

In order to use the internal coordinates, a first-order linear relation with Cartesian coordinates is normally adopted:[41]

$$\mathbf{s} - \mathbf{s}^0 = \mathbf{B}(\mathbf{x} - \mathbf{x}^0) \tag{5}$$

where the $\mathbf{s}$ and $\mathbf{x}$ column vectors are, respectively, the sets of internal (dimension $3N - 6$, where N is the number of atoms) and Cartesian (dimension $3N$) coordinates, $\mathbf{s}^0$ and $\mathbf{x}^0$ are the corresponding values for the reference structure and $\mathbf{B}$ is the Wilson matrix, which has dimensions $(3N - 6) \times 3N$. In general, the set of internal coordinates is not orthogonal, but a new orthogonal set can be defined as $\mathbf{s}' = \mathbf{G}^{1/2}\mathbf{s}$,[8] where $\mathbf{G} = \mathbf{B}^T\mathbf{m}^{-1}\mathbf{B}$ is the metric matrix and $\mathbf{m}$ is a $(3N \times 3N)$ diagonal matrix containing the atomic masses as diagonal elements.

Normal modes ($\mathbf{Q}$) in internal coordinates [$\mathbf{s} - \mathbf{s}^0 = \mathbf{L}\mathbf{Q}$, where $\mathbf{L}$ $((3N - 6) \times (3N - 6))$] can be obtained by means of the GF method,[41] after properly defining the Hessian matrix in internal coordinates ($\mathbf{F}$) from that in Cartesian ($\mathbf{H}_x$). It is worthy to notice that, in general, such transformation also involves the derivatives of the Wilson matrix with respect to the internal coordinates and the energy gradient in internal coordinates, but they both disappear at stationary points (AH model).[42,43]

Alternatively, internal normal modes can be obtained from those in mass-weighted Cartesian displacement coordinates which fulfill the Eckart conditions [$\mathbf{q} = \mathbf{T}\mathbf{Q}$, where $\mathbf{T}$ $(3N \times (3N - 6))$], as $\mathbf{L} = \mathbf{B}\mathbf{m}^{-1/2}\mathbf{T}$.[44] The above equation arises from an expression of $\mathbf{H}_x$ in terms of $\mathbf{F}$ that is only valid for stationary points, that is, only applicable for the AH model.

The Duschinsky matrix between the normal modes in Cartesian coordinates is $\mathbf{J}_{\mathrm{Cart}} = \mathbf{T}_g^t\mathbf{T}_e$, where $\mathbf{T}_g$ and $\mathbf{T}_e$ are the GS and ES mass-weighted Cartesian normal modes, respectively. Notice that before computing $\mathbf{J}_{\mathrm{Cart}}$, the initial and final structures need to be rotated so as to minimize the mixing of rotational coordinates by imposing the irrotational condition; we adopted the quaternion formalism.[45] However, even after aligning the ground- and excited-state structures, the Eckart conditions cannot be usually fulfilled simultaneously at both geometries due to axis switching effects,[46,47] and $\mathbf{J}_{\mathrm{Cart}}$ might not be exactly orthogonal. Naming $\mathbf{L}_g$ and $\mathbf{L}_e$ the GS and ES normal modes in internal coordinates, the corresponding Duschinsky matrix is[9] $\mathbf{J}_{\mathrm{Int}} = \mathbf{L}_g^{-1}\mathbf{L}_e$ or, following Reimers[8] and adopting orthogonal internal coordinates, $\mathbf{L}' = \mathbf{G}^{-1/2}\mathbf{L}$ and $\mathbf{L}'^t\mathbf{L}' = \mathbf{I}$, that is, the identity matrix,

$$\mathbf{J}_{\mathrm{Int}} = \mathbf{L}_g'^t\mathbf{G}_g^{-1/2}\mathbf{G}_e^{1/2}\mathbf{L}_e' \tag{6}$$

dx.doi.org/10.1021/ct4005849 | J. Chem. Theory Comput. XXXX, XXX, XXX−XXX

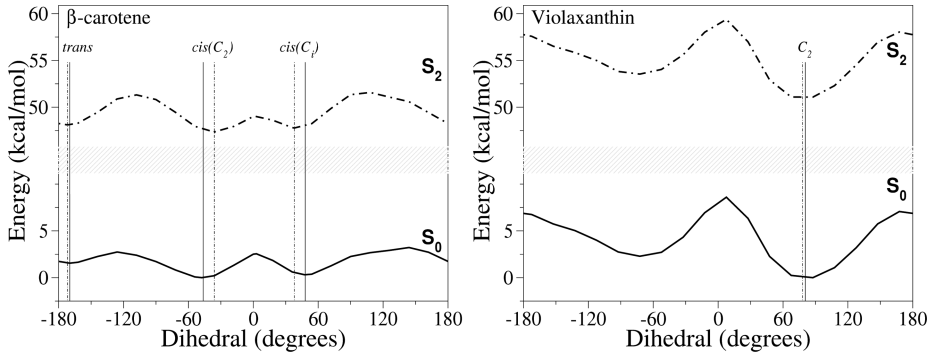

Figure 2. Potential energy plots generated by the scan around the dihedral connecting the ionone ring with the polyenic chain (D_{ring}) on the GS and ES PES computed at (TD)B3LYP/6-31G(d) level for β-carotene (left) and violaxanthin (right). Vertical lines indicate the location of the GS (straight) and ES (dashed) studied minima. The equivalent dihedral (D'_{ring}) was set to the lowest energy conformation.

From eq 6, it is clear that the Duschinsky matrix will be orthogonal only if the internal coordinates obtained at the reference geometries of the two electronic states share the same metric matrix, that is, if $\mathbf{G}_g = \mathbf{G}_e = \mathbf{G}$. Finally, within the AH model, the displacement vectors in mass-weighted Cartesian ($\mathbf{K}_{Cart}$) and internal[8] ($\mathbf{K}_{Int}$) coordinates are

$$\mathbf{K}_{Cart} = \mathbf{T}_g^t(\mathbf{q}_e^0 - \mathbf{q}_g^0) \tag{7}$$

$$\mathbf{K}_{Int} = \mathbf{T}_g^t \mathbf{m}^{-1/2} \mathbf{B}_g^T \mathbf{G}_g^{-1}(\mathbf{s}_e^0 - \mathbf{s}_g^0) \tag{8}$$

where $\mathbf{q}_g^0$ and $\mathbf{q}_e^0$, and $\mathbf{s}_g^0$ and $\mathbf{s}_e^0$, are respectively the mass-weighted Cartesian and internal coordinates at the reference structures. Notice also that equivalent expressions for $\mathbf{J}_{Int}$ and $\mathbf{K}_{Int}$ were derived by Borrelli et al. in ref 10. The previous expression highlights the connection of $\mathbf{K}_{Int}$ with $\mathbf{T}_g$ and $\mathbf{B}_g$ although it is worthy to realize that, as reported by Sharp,[9] $\mathbf{K}_{Int} = \mathbf{L}_g^{-1}(\mathbf{s}_e^0 - \mathbf{s}_g^0)$, so that it can be obtained without previously computing $\mathbf{T}_g$.

Moving from the representation of normal-modes in mass-weighted Cartesian coordinates to the one in internal coordinates, additional kinetic terms arise in the Hamiltonian (see for example ref 12), which becomes negligible in the limit of small displacements. In the present approach, in order to straightforwardly apply the TI and TD formulations developed for Cartesian normal modes, we neglected these terms.

For the VH model, information from the ES gradient is also required to estimate the displacement vector, whose evaluation, as well as that of the Duschinsky matrix have already been described elsewhere.[15,16] In this work, the models AH, with normal modes both in Cartesian, referred to as AH(Cartesian), and in internal coordinates, AH(internal), and VH have been used to evaluate the Duschinsky matrix and the displacement vector, in order to compute the Franck−Condon integrals needed to simulate the electronic spectra as detailed in the following section.

3. COMPUTATIONAL METHODS

The electronic PES of the ground and excited states have been computed by means of DFT and TD-DFT methods, which have been shown adequate to characterize both the ground state[48−50] and the targeted S_2 excited state[51−53] of carotenoids. We have used, concretely, the B3LYP density functional along with the double ξ with polarization for non-hydrogen atoms, 6-31G(d), basis set. In preliminary calculations for both β-carotene and violaxanthin, such combination of functional and basis set has been shown to reproduce the experimental spectrum line shape better than the CAM-B3LYP functional, although the whole spectrum is red-shifted around 0.4−0.5 eV. Since the main goal of this study is to evaluate the performance of different harmonic models to simulate the spectrum line shape, the effect of the DFT functional has not been investigated further.

In order to locate possible rotamers, for each carotenoid, both the GS and ES PESs have been preliminary explored by (TD)B3LYP/6-31G(d) relaxed scans along the dihedrals connecting the ionone rings with the polyenic chain. As observed in Figure 2, the GS has two minima for violaxanthin and three for β-carotene, and the same rotamers can be identified in the ES. For violaxanthin, we considered only the most stable minimum in further computations given the large energy difference that it has with the other minimum, while for β-carotene all minima were considered, that is, the two pseudo-*cis* minima with similar energy and the more energetic *trans* conformer. This latter structure was included in the study to further check the influence of the conformation on the spectroscopic features despite the fact that it is not expected to be populated in normal conditions. The selected structures were minimized at the ground and S_2 excited states using the (TD)B3LYP/6-31G(d) method.

For each rotamer, we computed the GS Hessian at the equilibrium geometry (FC), and the ES Hessian both at the FC point (to apply the VH model) and at its own minimum (to apply the AH model). Diagonalization of the Hessian provided the vibrational frequencies, which were all real when computed at the minimum and showed two imaginary frequencies at the FC point in the excited state for all the systems. These imaginary frequencies were replaced by their absolute values to allow the computation of the spectrum at harmonic level. Optimizations and subsequent Hessian evaluation were carried out *in vacuo*. Experimental spectra are recorded, however, in solvent, such as *n*-hexane or 3-methylpentane for β-carotene[31,54] and *n*-hexane, a mixture of ethanol, isopentane, and diethyl ether (EPA), or pyridine for violaxanthin.[26,29,55] For all the solvents, the spectrum at room temperature is available and shows a very similar shape. Since our main goal was to find an appropriate method to overcome the issues related with the structural displacement from GS to ES, we consider the results *in vacuo* qualitatively correct to make a comparison with the experimental spectrum.

Fully converged vibrationally resolved spectra were computed within the harmonic approximation including the possible differences of ground and excited state frequencies

dx.doi.org/10.1021/ct4005849 | J. Chem. Theory Comput. XXXX, XXX, XXX−XXX

and normal modes (Duschinsky effect).[13] We primarily adopted the time-dependent (TD) strategy, which is very well suited to efficiently obtain the vibronic spectra of medium-large molecules at finite temperature. A number of derivations of the correlation function χ (see eq 3) needed in TD calculations has been proposed in literature,[3,34,39,40,56−59] and they are indebted to seminal works by Kubo et al.[60] and the Mukamel's group;[61] we follow here the one given by Pollack and co-workers[34] (see also ref 2).

The TD simulations were complemented by TI calculations for low temperature spectra, in order to get detailed information on the most important stick transitions. To that end, we adopted the effective method, recently proposed by some of us[35,45,62] (implemented also in Gaussian 09),[63,64] based on partition of the possible vibronic transitions in classes C_n depending on the number n of simultaneously excited modes in the final state, and a prescreening technique to single out the important contributions of each class.

All the spectra calculations with either TI or TD strategies where performed using a developed version of the code *FClasses*.[65] TI spectra at 0 K were computed by considering C_1 and C_2 transitions with the maximum quantum number lower than 30 and 25, respectively, and setting the maximum number of integrals computed for each class to 10^9; for TD spectra the correlation function was computed with a time step of 0.24 fs for a total time of 1 ps. In both cases, the half-width at half-maximum (HWHM) of the convoluting Gaussian was set so as to better match the experimental width, which was 0.03 eV for β-carotene and 0.015 eV for violaxanthin. The electronic calculations were performed by using Gaussian 09 suite of programs.[66]

4. RESULTS

4.1. β-Carotene Isomers. Two of the three rotamers of β-carotene are very close to a *cis* dihedral configuration, and have C_i and nearly-C_2 symmetry, the latter being slightly above in energy. The third minimum correspond to a *trans* configuration, and its energy is around 1.5 kcal/mol above the *cis* minima. As for the experimental spectrum,[31] however, no information is given about the rotamers, and actually, a mixture of *cis* isomers might be present. Due to the low energy barrier between them, the Boltzmann relative populations are expected to be approximately 10:2 and 10:12 (*cis*-C_i:*cis*-C_2) at 77 and 300 K, respectively, taking into account that two degenerate nearly-C_2 conformers are predicted. Nevertheless, even at room temperature, the experimental spectrum does not display differentiated bands that could be assigned to each isomer. This can be a consequence of the limited resolution of the spectrum or may indicate that both species give rise to nearly the same spectra, which seems reasonable taking into account the similar structural features of the two species.

Optimizations at the (TD)B3LYP/6-31G(d) level show that the two distorted *cis* configurations display closely related structures, with the dihedral angles D_{ring} and D'_{ring}, which connect the β-ionone rings with the polyenic chain (see Figure 1), similarly deviating from the *cis* configuration (which corresponds to 0°). To get a general view of the conformational changes, we indicate in Figure 2 the value of one of the dihedrals (D_{ring}) on the corresponding scans for the S_0 and S_2 states. Specifically, for the C_i minimum $D_{ring} = -D'_{ring}$=47.6° in the ground state, and 36.0° in the excited state; for the nearly-C_2 minimum $D_{ring} \approx D'_{ring}$, with values changing from 47.4° and 47.8° in the ground state to 37.2° and 39.9° in the excited state; finally for the *trans* isomer the dihedrals, D_{ring} and D'_{ring}, correspond to nearly-*cis* and *trans* (i.e., 180°) configurations respectively, varying from 46.2° and −169.7° in the GS, to 36.1° and −171.7° in the ES. Comparing the three isomers, the sums of the absolute deviations of D_{ring} and D'_{ring} are 23.2°, 18.1°, and 12.1° for the *cis*-C_i, the *cis*-C_2, and *trans* isomers, respectively, which we use in the following as a qualitative measure of the structural displacement that occur in each case.

For the AH model, normal modes have been computed using Cartesian and internal coordinates, as indicated in Section 2. The simulation of the spectra has been carried out mainly with a TD approach, since TI methods revealed inefficient to provide fully converged spectra in most of the cases. For instance, the TI simulation of the *cis*-C_2 isomer at 10 K results in a very poor convergence, with the recovery of a fraction of 0.3 of the total FC intensity, and the shape of the spectrum is significantly different from the converged shape obtained using TD methods (Figure S1, in Supporting Information (SI)), evidencing the potential risk of considering reliable low-converged spectra. Interestingly, this issue is alleviated when internal coordinates are used, reaching a convergence of 0.6. This indicates that the low convergence is a symptom, in part, of the failure of the Cartesian coordinates approach, as described below. Furthermore, even in those cases where TI could afford a nearly converged spectrum, the time required for the TD approach is significantly shorter, as observed in Table S1 in SI, where CPU times required by each approach are compared for some systems.

4.1.1. cis-C_i Isomer of β-Carotene. The spectra obtained using the TD approach at 77 and 300 K are plotted in Figure 3,

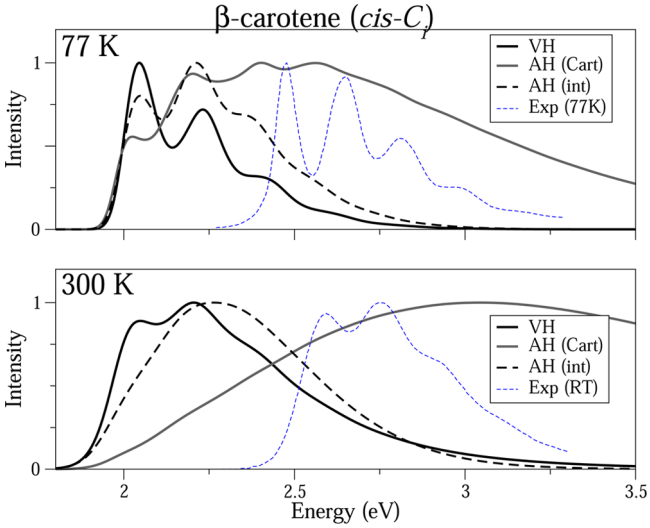

Figure 3. Simulated spectrum of the *cis*-C_i conformer of β-carotene at 77 and 300 K *in vacuo* using VH, AH(Cartesian) and AH(internal) models and (TD)B3LYP/6-31G(d) calculations. The experimental spectrum from Jailaubekov et al.[31] in 3-methylpentane is included for comparison.

showing that for the AH model the internal coordinates description is able to reproduce correctly the width of the experimental spectrum in contrast with the Cartesian coordinates description which strongly overestimates it.

Although the AH(internal) model gives a reasonable prediction of the spectral width, it does not reproduce correctly the relative intensity of the experimental vibronic bands.[31] The spectrum obtained using the VH model, on the contrary, gives

dx.doi.org/10.1021/ct4005849 | J. Chem. Theory Comput. XXXX, XXX, XXX−XXX

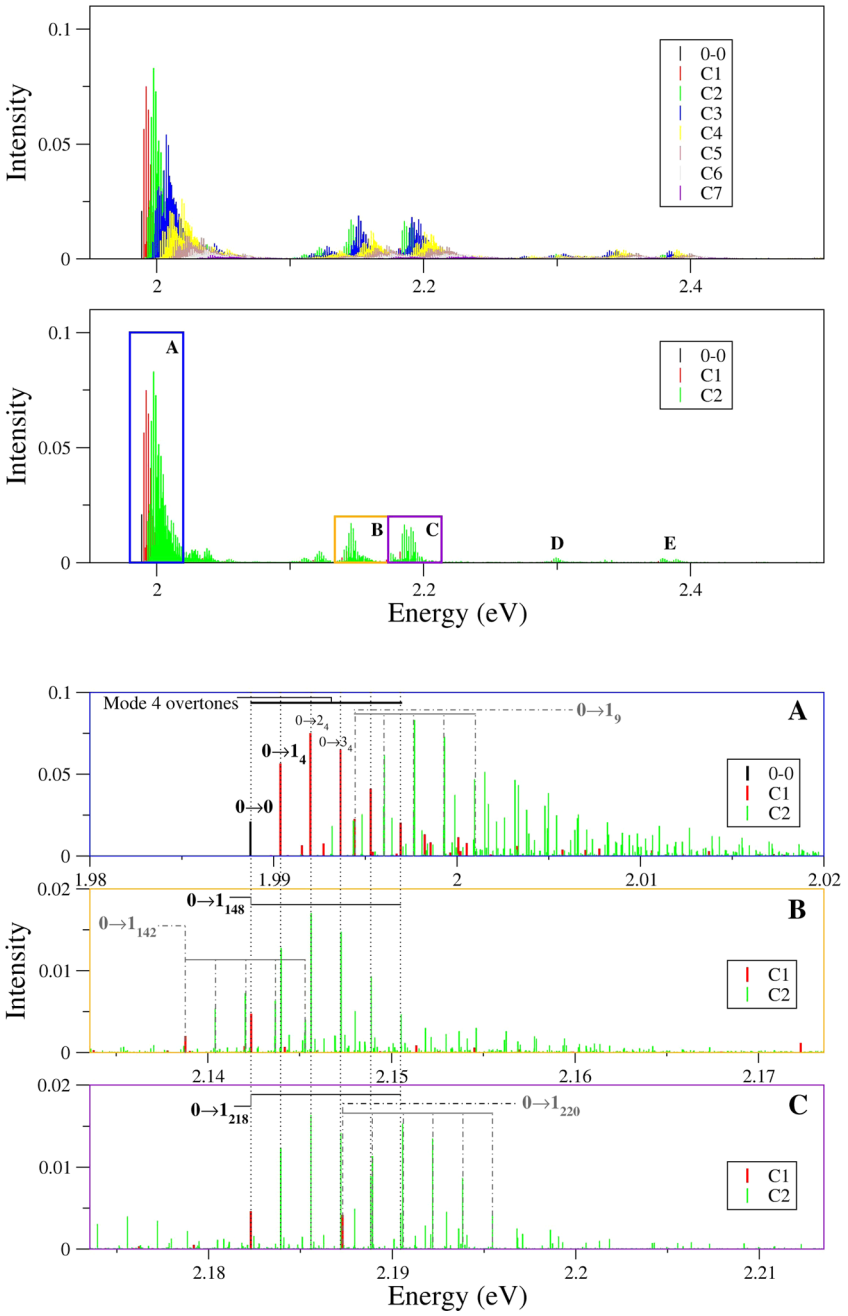

Figure 4. TI spectrum at 0 K (recovered 0.53 fraction), computed using internal coordinates. Contributions for all the computed *classes* are shown (top), and the selected regions with only C_0 (0−0) to C_2 *classes* transitions are indicated. A zoom on these regions is shown on the bottom panels.

the right broadening and relative intensities, at both 77 and 300 K. Indeed, although Cartesian coordinates are used in the VH, this latter approach does not share the same issues with AH model, since the normal modes of the ground and excited states are computed at the same structure, that of the GS minimum. A drawback of the adoption of the VH model is that, as we anticipated above, the ES Hessian at the FC point can exhibit some imaginary frequencies, and this actually happens for two modes in the *cis*-C_i isomer: $\nu_1^{\text{imag}} = 31.17i$ cm^{-1} and $\nu_2^{\text{imag}} = 25.15i$ cm^{-1}. Following previous works,[15] we have bypassed this problem by assigning to such frequencies an arbitrary real value, namely the modulus of the imaginary number, thus retaining the harmonic description of the system. This procedure is certainly arbitrary, and its consequences were investigated in SI, by systematically changing the frequencies in a range between 10 and 90 cm^{-1}. It is shown that the main vibronic structure of the spectrum is not altered, while the actual choice of the real frequency does change the relative height of the peaks (see Figure S2, in SI). This fact introduces some unreliability, although the general trends are kept. An anharmonic treatment of the modes featuring imaginary frequencies is nevertheless scoped for future approaches.

Assignment of the Main Bands. A more detailed analysis of the spectrum can be obtained by assigning the most relevant stick bands obtained by a TI calculation at $T = 0$ K. The simulated TI spectrum according to the AH(internal) model, reported in Figure 4, recovers a 0.53 fraction of the full FC spectrum, but is perfectly adequate to analyze the most intense vibronic transitions, showing that they all belong to the C_1−C_3 classes. More specifically, the bands of the most intense

dx.doi.org/10.1021/ct4005849 | J. Chem. Theory Comput. XXXX, XXX, XXX−XXX

progression are associated with overtones of ES mode 4 (i.e., 0 → 1_4, 0 → 2_4, 0 → 3_4, ...). The main contribution to this mode comes from the torsion angles D_{ring} and D'_{ring}, that are, in fact, significantly displaced from GS to ES. This analysis also highlights that this progression, arising from the displacement of the aforementioned dihedral angles, constitutes an intrinsic source of broadening of the spectrum.

Progressions of the mode 4 are identified all over the spectrum, in combination with excitation along other modes. Regarding the low energy region of the spectrum, the most relevant C_2 bands combine excitations along mode 4 with 0 → 1_9, 0 → 2_9, 0 → 1_7, 0 → 1_5, and 0 → 1_{13} transitions. Interestingly, mode 9 also shows a significant contribution of the D_{ring} dihedral. The strongest C_3 transitions correspond to combinations of two fundamentals of modes 5, 7, 9, and 13, together with the mode 4 progression. Focusing on the more energetic part of the spectrum, the most relevant bands are the fundamentals 0 → 1_{148}, 0 → 1_{142}, 0 → 1_{218} and 0 → 1_{220}, which mainly correspond to C−C stretching and C−C−H bending motions along the conjugated chain. As expected, in the same energy window the most intense C_3 bands involve the excitation of these high-frequency modes together with mode 4 and another among the low-frequency modes (5, 7, 9) showing strong fundamentals.

Cause of the Failure of AH(Cartesian) Model. We have selected the *cis*-C_i isomer to investigate the cause of the overestimation of the spectral width obtained using the AH (Cartesian) model. To that end, we performed two additional simulations, one replacing the ES Hessian by that of the ground state, which implies setting the Duschinsky matrix equal to the identity matrix, i.e. using Adiabatic Shift (AS) model,[15] and the other setting all the displacements to zero, which is referred to as the Zero-Displacement (ZD) calculation. These computations allow to disentangle the effect of the normal mode displacements and of the Duschinsky matrix on the spectrum. Calculations using the AS model (see Figure S3, in the Supporting Information, for details) show that the displacements predicted by the AH(Cartesian), AH(internal), and VH models, which are represented in Figure S4 in SI, induce very similar broadenings when going from 77 to 300 K. It is also worth noticing that, with all the models, the most largely displaced modes are those related with the D_{ring} dihedral coordinate (see SI Table S2).

On the contrary, ZD spectra clearly evidence an anomalous behavior of the AH (Cartesian) model, (see Figure S5, in SI) allowing us to state that the main cause of the excessive width of the AH (Cartesian) spectra can be traced back to inaccuracies in the Duschinsky matrix. In order to single out the vibronic transitions responsible for such erroneous broadening, ZD simulations using AH (Cartesian) model were also carried out with TI approach at low temperature (10 K). The ZD spectrum in Figure 5 exhibits a single vibronic band (at ≈2.0 eV) for VH and AH (internal) approaches, while two additional vibronic features at ≈2.5 eV are seen according to the AH (Cartesian) model. These two bands are the ones responsible for the erroneous width of the AH (Cartesian) spectrum and are due to C_2 transitions (see Figure 5) involving the simultaneous excitation of low- (torsions) and high- (bond stretching, and in particular CH-stretching, i.e., modes from 227 to 282) frequency modes, as shown in Table S3, in the Supporting Information. It is worthy to remark that, in ZD spectra, such combinations can only arise from Duschinsky mixing. In order to further analyze the origin of these bands, we

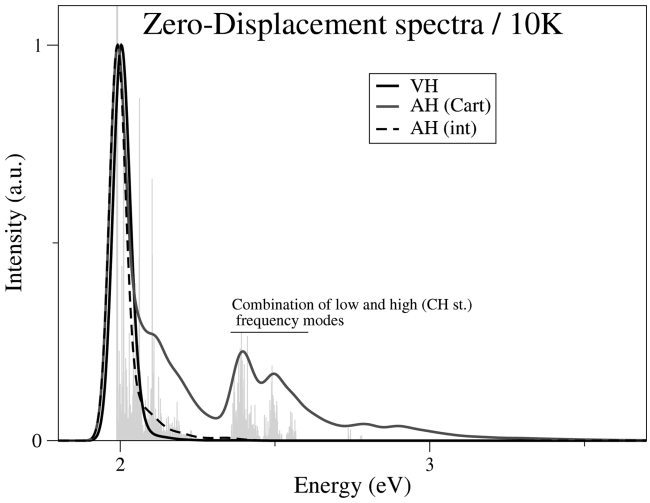

Figure 5. Simulated spectrum of *cis*-C_i conformer of β-carotene at 10 K using the Duschinsky matrix evaluated with AH(Cartesian), AH(internal), and VH models, with B3LYP/6-31G(d) computed Hessian, and neglecting all displacements (zero-displacement). Transitions computed using TI methods are included for the AH (Cartesian) model (gray bars).

have taken a closer look to the Duschinsky matrices obtained with either AH(Cartesian), AH(internal), or VH models, whose bidimensional representations are given in Figure S6 in the SI. From this figure, it is evident that all the three models predict a diffuse pattern of Duschinsky couplings, with some (expected) tendency to form diagonal blocks. However, the AH(Cartesian) model additionally exhibits appreciable couplings between high-frequency CH normal modes and low-frequency ones, that are practically vanishing according to AH(internal) and VH models. This observation strengthens the results of the analysis of the stick vibronic transitions given above, indicating that these spurious couplings are the cause of the anomalous behavior of the AH(Cartesian) model. In conclusion, the excessive broadening obtained with the AH (Cartesian) is due to C_2 combination bands caused by Dushinsky couplings and it arises as a consequence of a deficient description of curvilinear low frequency modes in Cartesian coordinates, leading to erroneous C−H bond stretchings at large curvilinear displacements. Both AH (internal) and VH models fix this issue.

Analysis of the Duschinsky matrix with the internal representation in Figure S6 of the SI also points out significant mixings of the low frequency normal modes of the GS and the high frequency modes (excluding the CH ones) of the ES, which are not observed in VH model. These couplings are likely connected with the differences observed between the AH(internal) and VH spectra, shown in Figure 3. The AH(internal) one exhibits a higher intensity of the second vibronic peak at about ≈2.2 eV and a more significant loss of the vibronic resolution at room temperature. Interestingly, these mixings involve motions along dihedral angles that, as shown in Section 4.3, are directly connected to the appearance of nonorthogonality issues in the Duschinsky matrix.

4.1.2. cis-C_2 Conformer. The spectra obtained for the *cis* -C_2 conformer are shown in Figure 6, at 77 and 300 K. As it happens, in the case of the *cis*-C_i conformer, the AH(internal) model corrects the excessively broad spectrum obtained in Cartesian coordinates. Actually, the spectrum obtained with the AH(internal) model is, in this case, very similar to the

dx.doi.org/10.1021/ct4005849 | J. Chem. Theory Comput. XXXX, XXX, XXX−XXX

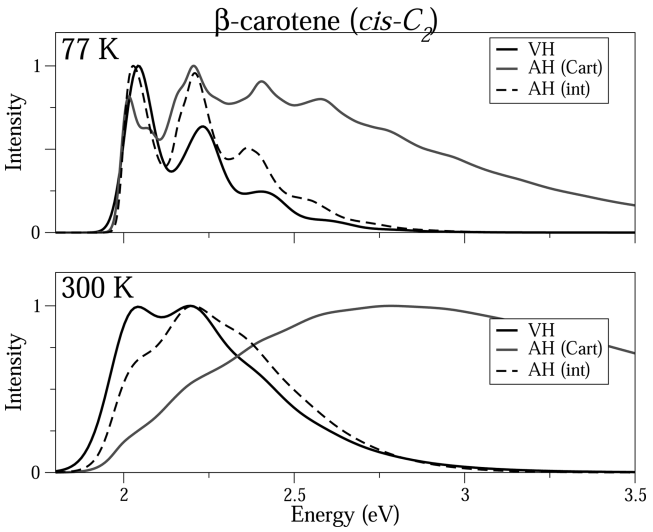

Figure 6. Simulated spectrum of the *cis*-nearly-C_2 conformer of β-carotene at 77 and 300 K *in vacuo* using VH, AH(Cartesian) and AH(internal) models and (TD)B3LYP/6-31G(d) calculations.

experimental one at 77 K, while the relative intensity of the bands at 300 K does not follow the experiment. Also in this system the shape of the VH spectrum reasonably agrees with the experimental one, although at 77 K the high energy region is significantly underestimated.

4.1.3. trans Isomer. The spectra for the *trans* isomer at 77 and 300 K are shown in Figure 7, including the experimental

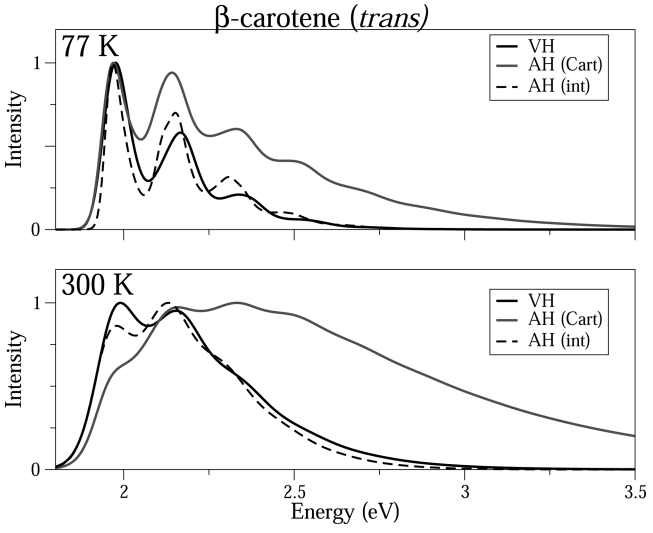

Figure 7. Simulated spectrum of the *trans* conformer of β-carotene at 77 and 300 K *in vacuo* using VH, AH(Cartesian) and AH(internal) models and (TD)B3LYP/6-31G(d) calculations.

spectrum as a reference, although this isomer is not expected to significantly contribute to the experimental line shape. As it happens for the other isomers, the simulated spectrum obtained using the AH model in Cartesian coordinates appears to be too broad, although the anomalous effect is less significant as compared with the *cis* isomers. This difference can be directly related with the smaller structural displacement from GS to ES minima, which can also explain the similarities between the AH(internal) and VH models.

4.2. Violaxanthin. In this section, we analyze the spectrum of violaxanthin by only focusing on the lowest minimum in the PES. In this case, the two dihedrals connecting the ionone ring with the polyenic chain are equal due to the C_2 symmetry, and they change from 80.6° in the GS to 78.2° in the ES. The sum of both displacements is 4.8°, that is, significantly smaller than the displacement in β-carotene. Experimental spectra of violaxanthin have been reported at 77 K and room temperatures in EPA and pyridine.[26,29] These spectra are much better resolved than those for β-carotene. This is most likely due to the smaller structural displacement associated with the D_{ring} dihedral, in connection with the broadening effect of the low-frequency modes progressions identified in Section 4.1.1 for β-carotene.

The simulated and experimental spectra for violaxanthin are shown in Figure 8. As observed, the B3LYP computed spectra

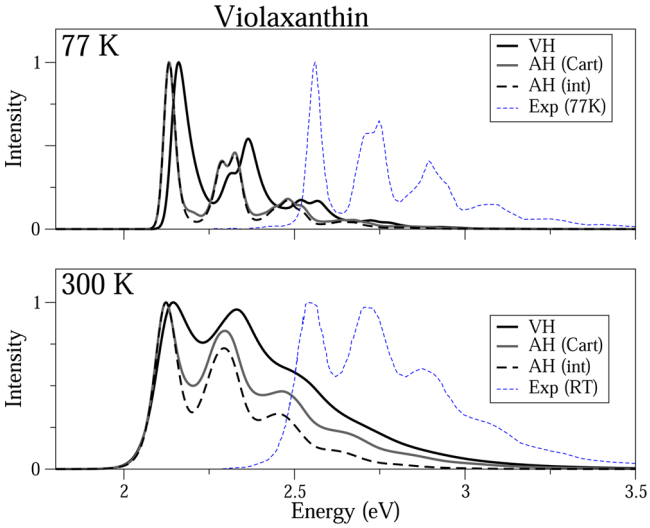

Figure 8. Simulated spectrum of violaxanthin at 77 and 300 K *in vacuo* using VH, AH(Cartesian), and AH(internal) models and B3LYP/6-31G(d) calculations. The experimental spectrum from Cong et al.[29] in EPA (77 K) and pyridine (RT) is included for comparison.

are red-shifted by ≈0.4 eV, as occurs in β-carotene. Due to the small structural displacement, the spectrum obtained using the AH(Cartesian) model displays the correct width, with a line shape very similar to that provided by the AH(internal) model, and both are in good agreement with experiment at low temperatures. Indeed, in this case the AH model perform slightly better than the VH model, although at high temperatures the AH spectrum underestimates the intensity in the high energy region. The most relevant discrepancy between the two AH models lies around 2.2 eV, where a shoulder appears using Cartesian coordinates, which disappears when internal coordinates are used. This peak is not experimentally observed and is due to the same artifact discussed for β-carotene, as evidenced by the ZD spectrum at 10 K (Figure S7 of the SI), which shows spurious combination bands, although much less intense than in β-carotene. At 300 K, all models underestimate the spectrum at high energies, although the overall shape seems to be better reproduced by the AH models (see the relative intensity of the second and third bands, and the excessive broadening of the VH spectrum). In analogy with the previous cases, the more intense high-energy wing predicted by the AH (Cartesian) model, as

dx.doi.org/10.1021/ct4005849 | J. Chem. Theory Comput. XXXX, XXX, XXX−XXX

compared with that provided by the AH (internal) model, is due to combination bands (see Figure S7).

4.3. Nonorthogonality of the Duschinsky Matrix in Internal Coordinates. As we discussed in Section 2, the Duschinsky matrix in internal coordinates is in general nonorthogonal. In this last section, we check the extent of this phenomenon for the investigated systems by analyzing the difference of the matrix $\mathbf{D} = \mathbf{G}_1^{-1/2}\mathbf{G}_2^{1/2}$ (see eq 6) from the identity matrix **I**, with the scope to figure out if nonorthogonality issues increase with the distortion of the molecule following the electronic transition, if they manifest also on the $\mathbf{J}_{Int}$ determinant, and if they are preferentially connected to specific modes. This analysis is interesting *per se* inasmuch a nonorthogonal $\mathbf{J}_{Int}$ requires the inclusion of a normalization factor $\det(\mathbf{J}_{Int})^{-1/2}$ in the calculation of FC factors[9] and it will reveal that nonorthogonality is directly connected to the torsional degrees of freedom that undergo larger displacements. Moreover, though there is no direct relation between the nonorthogonality of $\mathbf{J}_{iInt}$ and the relevance of the extra-kinetic terms in the Hamiltonian in internal coordinates[12] we neglected, it is suggestive to notice that such terms arise from the dependence of the **G** matrix on the internal coordinates, and that, on the same foot if $\mathbf{G}_1 = \mathbf{G}_2$ (that is, if the **G** matrix does not change from the initial- to the final-state equilibrium geometry), $\mathbf{J}_{Int}$ becomes orthogonal. In Table 1, we give the values of some key parameters of matrix **D**, which is represented through bidimensional plots in Figure S8 in Supporting Information. As shown in Table 1, the value of the matrix determinant is in all the cases close to the ideal value 1, independently of the GS→ES displacement. Surprisingly, the worst value is actually obtained for the system that exhibits the smallest structural displacement (violaxanthin). An analysis of the whole **D** matrix shows that the largest deviations from the identity matrix occur for the elements related to the dihedral angles that describe the torsions along the conjugated chain. Figure S8 in SI shows that differences become more significant as the structural displacements from GS to ES increase, the ordering being β-carotene (*cis* $-C_i$) $\gtrsim$ β-carotene (*cis* $-C_2$) > β-carotene (*trans*) > violaxanthin. For the other parameters highlighted in Table 1, it is observed that, although the trace of **D** gives the correct value, appreciable deviations from the unity occur for some diagonal elements and such fluctuations are almost identical for all the systems, regardless the extent of the GS/ES displacement. Concerning the off-diagonal terms, the deviations from a pure identity matrix are more significant for the systems with a larger structural displacement, with the lowest mean absolute off-diagonal terms corresponding therefore to violaxanthin. Interestingly, the extent of the deviation of **D** from the ideal values depends, as shown in Table 1, on the choice of the set of coordinates: concretely, if equivalent internal elements are chosen in the two states, **D** is closer to unity. The nice agreement between Cartesian and internal coordinates for violaxanthin agrees well with the fact that the **D** matrix for this system is very close to the unit matrix. For the other systems, the deviations of the **D** matrix are more significant, although it is still close to the identity matrix. Together with what already known from literature,[12,67] the observed direct relationship between the deviation of **D** from the identity matrix and the extent of the structural displacements from GS to ES minima suggests that further work is necessary to investigate the reliability of the use of internal coordinates in association with harmonic approximation and simplified kinetic Hamiltonians for very large displacements.

Table 1. Representative Values of $\mathbf{D} = \mathbf{G}_1^{-1/2}\mathbf{G}_2^{1/2}$ Matrix for the $S_0 \rightarrow S_2$ Transition of β-Carotene and Violaxanthin, Using Internal Coordinates Sets[a]

	det[b]	trace	min diag[c]	max diag[d]	MAD off-diag[e]	avg. |off-diag|[f]
			β-Carotene			
ideal	1	282	1	1	0	0
cis-C_i(E)	1.003	282.27	0.83	1.13	0.25	2.1×10^{-3}
cis-C_i(R)	1.014	282.28	0.82	1.13	0.37	1.8×10^{-3}
cis-C_2(E)	0.999	282.18	0.81	1.14	0.23	1.8×10^{-3}
cis-C_2(R)	1.010	282.19	0.80	1.14	0.25	1.5×10^{-3}
trans(E)	0.999	282.11	0.83	1.12	0.24	1.4×10^{-3}
trans(R)	1.001	282.11	0.83	1.12	0.24	1.2×10^{-3}
			Violaxanthin			
ideal	1	294	1	1	0	0
C_2(E)	0.968	294.00	0.83	1.14	0.14	7.2×10^{-4}
C_2(R)	0.979	294.01	0.83	1.22	0.22	7.2×10^{-4}

[a]For every system, internal coordinates have been selected either randomly (R) or including equivalent bonds, angles and dihedrals (E). [b]Matrix determinant. [c]Minimum value of diagonal terms. [d]Maximum value of diagonal terms. [e]Maximum absolute deviation from zero of off-diagonal terms. [f]Average absolute value of off-diagonal terms.

5. CONCLUSIONS

In this work we have tackled the problem of defining a proper and efficient computational protocol to simulate vibrationally resolved electronic spectra at room temperature in sizable systems exhibiting large-amplitude deformations. We focused on the $S_0 \rightarrow S_2$ band of β-carotene (96 atoms) and violaxanthin (100 atoms), testing different models based on the harmonic approximation, including AH, using both Cartesian and internal coordinates, and VH. These carotenoids exhibit different extents of conformational displacement from GS to ES minima, qualitatively reported by the change of the dihedral angle connecting the ionone rings with the polyenic chain and ranging from small displacements for violaxanthin to rather large ones for the different β-carotene isomers This allows therefore a complete investigation on how such structural displacement affects the efficiency and accuracy of the models under study.

For the *cis*-C_i and *cis*-C_2 isomers of β-carotene, which display relatively large structural displacements, the AH model in Cartesian coordinate remarkably fails to reproduce the experimental spectrum, predicting a excessively broad band. This problem arises from the poor description of the curvilinear displacements given by the Cartesian coordinates, which affect the evaluation of the Duschinsky matrix, and it is fixed when internal coordinates are used. The VH model also performs quite well, providing a comparable, or even slightly better simulation of the experimental line shapes, at both low and room temperatures. The failure of AH(Cartesian) model is less significant for the *trans* isomer of β-carotene due to the smaller displacement from GS to ES minima, performing in this case closer to the AH(internal) and VH models. For violaxanthin the structural displacement is rather small, and consequently, AH(Cartesian) gives almost identical spectra as compared with AH(internal) at low temperatures, although some differences still appear at high temperatures due to residual spurious couplings in Cartesian coordinates. Interestingly, for this molecule, the spectra simulated using both AH models are better that those obtained using the VH model.

dx.doi.org/10.1021/ct4005849 | J. Chem. Theory Comput. XXXX, XXX, XXX−XXX

In internal coordinates the $\mathbf{G}_1^{-1/2}\mathbf{G}_2^{1/2}$ product matrix controls the orthogonality of the Duschinsky matrix.[8] Our results show that, although some appreciable deviations from the unity are observed for $\mathbf{G}_1^{-1/2}\mathbf{G}_2^{1/2}$, orthogonality is almost preserved in the investigated cases but deviations are more significant for larger structural displacements.

At a more chemical level, we have obtained vibronic spectra for β-carotene and violaxanthin, in good agreement with experiment, using DFT PES. Concretely, the temperature effects on the spectrum resolution were very well described. In the case of β-carotene, the study of different rotamers suggest that the different conformers might be differentiated by the characteristic spectroscopic signature for the $S_0 \rightarrow S_2$ transition and, for instance, a more intense first vibronic band would appear in the *trans* isomer, although the lack of experimental data and the residual difference of the AH(internal) and VH spectra prevent a rigorous statement.

As a more general comment, in agreement with previous works on smaller systems,[11,12] the present study shows that by adopting internal coordinates, even spectra of systems undergoing large-amplitude displacements can become amenable (to a given extent) of a description in terms of harmonic PESs. When coupled with TD computational strategies, this further extends the wealth of molecules for which a reliable description of the vibronic spectra, including the effects of all the nuclear coordinates is now at hand. More precisely, the usage of internal coordinates allows us to disentangle the problems due to the intrinsic limitation of harmonic approximation, from those arising when one tries to describe a remarkable distortion along a curvilinear coordinate in terms of rectilinear displacements. As intuitive, our analysis highlights that these distortions mainly appear as artificial couplings between the rectilinear modes. Ensuring the best separation (smallest couplings) among the modes, an internal coordinate framework is also the best suited for setting up hybrid models where the PES is harmonic along most of the coordinates, apart from a few of them that are treated at anharmonic level.[10,11,68]

Finally, if a harmonic approach in Cartesian coordinates needs to be selected also for systems with large-amplitude displacements, our results indicate that VH model should be preferred over the AH one, since the problems in the definition of the Duschinsky matrix are strongly reduced by the usage of the same reference geometry for the initial and the final states. However, one should be aware that the frequent appearance of small imaginary frequencies, *de facto* irrelevant in many cases,[15,69] can affect specific spectral features (like the relative intensity of the vibronic bands).

■ ASSOCIATED CONTENT

Supporting Information

Table and figure illustrating the performance of TD and TI approaches. VH spectra for β-carotene setting the two imaginary frequencies to different values. For the *cis*-C_i isomer of β-carotene: figure showing the AS spectra and table with the most largely displaced modes computed at AH(Cartesian), AH(internal), and VH models; figure with the ZD spectra and table with the most relevant transitions; figure reporting the displacements along all the modes and table highlighting the largest ones; bidimensional plots of the Dushinsky matrix. ZD spectra for violaxanthin at 10 K. Bidimensional plot representing the **D** matrices for all the systems. This material is available free of charge via the Internet at http://pubs.acs.org.

■ AUTHOR INFORMATION

Corresponding Authors

*E-mail: jcb1@um.es.

*E-mail: fabrizio.santoro@iccom.cnr.it.

Notes

The authors declare no competing financial interest.

■ ACKNOWLEDGMENTS

This work was partially supported by the Spanish Ministerio de Ciencia e Innovación under Projects CTQ2011-25872 and CONSOLIDER CSD2009-00038, by the Fundación Séneca del Centro de Coordinación de la Investigación de la Región de Murcia under Project 08735/PI/08, and by Italian MIUR (FIRB Futuro in Ricerca RBFR10Y5VW and PRIN 2010-2011 2010ERFKXL). J.C. acknowledges a FPU fellowship provided by the Ministerio de Educación of Spain and also thanks ICCOM-CNR (Pisa) for hospitality during a three month stay funded by the FPU program. F.A. acknowledges support from EU People Program, Marie Curie Actions (grant agreement No. 246550).

■ REFERENCES

(1) Biczysko, M.; Bloino, J.; Santoro, F.; Barone, V. In *Time-Independent Approaches to Simulate Electronic Spectra Lineshapes: From Small Molecules to Macrosystems*; Barone, V., Ed.; John Wiley & Sons, Inc.: New York, 2011; Chapter 8, pp 361−443.

(2) Lami, A.; Santoro, F. In *Time-Dependent Approaches to Calculation of Steady-State Vibronic Spectra: From Fully Quantum to Classical Approaches*; Barone, V., Ed.; John Wiley & Sons, Inc.: New York, 2011; Chapter 10, pp 475−516.

(3) Huh, J.; Berger, R. Coherent state-based generating function approach for Franck−Condon transitions and beyond. *J. Phys.: Conf. Ser.* **2012**, *380*, 012019.

(4) Borrelli, R.; Capobianco, A.; Peluso, A. Franck−Condon factors—Computational approaches and recent developments. *Can. J. Chem.* **2013**, *91*, 495−504.

(5) Tomasi, J.; Mennucci, B.; Cammi, R. Quantum mechanical continuum solvation models. *Chem. Rev.* **2005**, *105*, 2999−3094.

(6) Bloino, J.; Barone, V. A second-order perturbation theory route to vibrational averages and transition properties of molecules: General formulation and application to infrared and vibrational circular dichroism spectroscopies. *J. Chem. Phys.* **2012**, *136*, 124108.

(7) Cappelli, C.; Bloino, J.; Lipparini, F.; Barone, V. Toward ab initio anharmonic vibrational circular dichroism spectra in the condensed phase. *J. Phys. Chem. Lett.* **2012**, *3*, 1766−1773.

(8) Reimers, J. R. A practical method for the use of curvilinear coordinates in calculations of normal-mode-projected displacements and Duschinsky rotation matrices for large molecules. *J. Chem. Phys.* **2001**, *115*, 9103−9109.

(9) Sharp, T. E.; Rosenstock, H. M. Franck−Condon factors for polyatomic molecules. *J. Chem. Phys.* **1964**, *41*, 3453−3463.

(10) Borrelli, R.; Peluso, A. The vibrational progressions of the N → V electronic transition of ethylene: A test case for the computation of Franck−Condon factors of highly flexible photoexcited molecules. *J. Chem. Phys.* **2006**, *125*, 194308.

(11) Borrelli, R.; Peluso, A. The electron photodetachment spectrum of c-$C_4F_8^-$: A test case for the computation of Franck−Condon factors of highly flexible molecules. *J. Chem. Phys.* **2008**, *128*, 044303.

(12) Capobianco, A.; Borrelli, R.; Noce, C.; Peluso, A. Franck−Condon factors in curvilinear coordinates: The photoelectron spectrum of ammonia. *Theor. Chem. Acc.* **2012**, *131*, 1−10.

(13) Duschinsky, F. On the interpretation of electronic spectra of polyatomic molecules. I. The Franck−Condon principle. *Acta Physicochim.: URSS* **1937**, *7*, 551−566.

(14) Cederbaum, L. S.; Domcke, W. A many-body approach to the vibrational structure in molecular electronic spectra. I. Theory. *J. Chem. Phys.* **1976**, *64*, 603−611.
(15) Avila Ferrer, F. J.; Santoro, F. Comparison of vertical and adiabatic harmonic approaches for the calculation of the vibrational structure of electronic spectra. *Phys. Chem. Chem. Phys.* **2012**, *14*, 13549−13563.
(16) Hazra, A.; Chang, H. H.; Nooijen, M. First principles simulation of the UV absorption spectrum of ethylene using the vertical Franck−Condon approach. *J. Chem. Phys.* **2004**, *121*, 2125−2136.
(17) Domcke, W.; Cederbaum, L.; Köppel, H.; von Niessen, W. A comparison of different approaches to the calculation of Franck−Condon factors for polyatomic molecules. *Mol. Phys.* **1977**, *34*, 1759−1770.
(18) Cesar, A.; gren, H. A.; de Brito, A. N.; Svensson, S.; Karlsson, L.; Keane, M. P.; Wannberg, B.; Baltzer, P.; Fournier, P. G.; Fournier, J. Vibronic and electronic states of doubly charged H[sub 2]S studied by Auger and charge transfer spectroscopy and by ab initio calculations. *J. Chem. Phys.* **1990**, *93*, 918−931.
(19) Nooijen, M. Investigation of Herzberg−Teller Franck−Condon approaches and classical simulations to include effects due to vibronic coupling in circular dichroism spectra: The case of dimethyloxirane continued. *Int. J. Quantum Chem.* **2006**, *106*, 2489−2510.
(20) Lin, N.; Santoro, F.; Rizzo, A.; Luo, Y.; Zhao, X.; Barone, V. Theory for vibrationally resolved two-photon circular dichroism spectra. Application to (R)-(+)-3-methylcyclopentanone. *J. Phys. Chem. A* **2009**, *113*, 4198−4207.
(21) Cogdell, R. J.; Frank, H. A. How carotenoids function in photosynthetic bacteria. *Biochim. Biophys. Acta, Rev. Bioenerg.* **1987**, *895*, 63−79.
(22) Polívka, T.; Sundström, V. Ultrafast dynamics of carotenoid excited states—From solution to natural and artificial systems. *Chem. Rev.* **2004**, *104*, 2021−2072.
(23) Polívka, T.; Sundström, V. Dark excited states of carotenoids: Consensus and controversy. *Chem. Phys. Lett.* **2009**, *477*, 1−11.
(24) Götze, J. P.; Thiel, W. TD-DFT and DFT/MRCI study of electronic excitations in Violaxanthin and Zeaxanthin. *Chem. Phys.* **2013**, *415*, 247−255.
(25) Sugisaki, M.; Yanagi, K.; Cogdell, R. J.; Hashimoto, H. Unified explanation for linear and nonlinear optical responses in β-carotene: A sub-20-fs degenerate four-wave mixing spectroscopic study. *Phys. Rev. B* **2007**, *75*, 155110.
(26) Josue, J. S.; Frank, H. A. Direct determination of the S1 excited-state energies of xanthophylls by low-temperature fluorescence spectroscopy. *J. Phys. Chem. A* **2002**, *106*, 4815−4824.
(27) Niedzwiedzki, D. M.; Sullivan, J. O.; Polívka, T.; Birge, R. R.; Frank, H. A. Femtosecond time-resolved transient absorption spectroscopy of xanthophylls. *J. Phys. Chem. B* **2006**, *110*, 22872−22885.
(28) Niedzwiedzki, D.; Koscielecki, J. F.; Cong, H.; Sullivan, J. O.; Gibson, G. N.; Birge, R. R.; Frank, H. A. Ultrafast dynamics and excited state spectra of open-chain carotenoids at room and low temperatures. *J. Phys. Chem. B* **2007**, *111*, 5984−5998.
(29) Cong, H.; Niedzwiedzki, D. M.; Gibson, G. N.; Frank, H. A. Ultrafast time-resolved spectroscopy of xanthophylls at low temperature. *J. Phys. Chem. B* **2008**, *112*, 3558−3567.
(30) Amarie, S.; Förster, U.; Gildenhoff, N.; Dreuw, A.; Wachtveitl, J. Excited state dynamics of the astaxanthin radical cation. *Chem. Phys.* **2010**, *373*, 8−14.
(31) Jailaubekov, A. E.; Vengris, M.; Song, S.-H.; Kusumoto, T.; Hashimoto, H.; Larsen, D. S. Deconstructing the excited-state dynamics of β-carotene in solution. *J. Phys. Chem. A* **2011**, *115*, 3905−3916.
(32) Kurashige, Y.; Nakano, H.; Nakao, Y.; Hirao, K. The $\pi \rightarrow \pi^*$ excited states of long linear polyenes studied by the CASCI-MRMP method. *Chem. Phys. Lett.* **2004**, *400*, 425−429.
(33) Kleinschmidt, M.; Marian, C. M.; Waletzke, M.; Grimme, S. Parallel multireference configuration interaction calculations on mini-β-carotenes and β-carotene. *J. Chem. Phys.* **2009**, *130*, 044708.
(34) Ianconescu, R.; Pollak, E. Photoinduced cooling of polyatomic molecules in an electronically excited state in the presence of Dushinskii rotations. *J. Phys. Chem. A* **2004**, *108*, 7778−7784.
(35) Santoro, F.; Lami, A.; Improta, R.; Barone, V. Effective method to compute vibrationally resolved optical spectra of large molecules at finite temperature in the gas phase and in solution. *J. Chem. Phys.* **2007**, *126*, 184102.
(36) Dierksen, M.; Grimme, S. An efficient approach for the calculation of Franck−Condon integrals of large molecules. *J. Chem. Phys.* **2005**, *122*, 244101.
(37) Jankowiak, H.-C.; Stuber, J. L.; Berger, R. Vibronic transitions in large molecular systems: Rigorous prescreening conditions for Franck−Condon factors. *J. Chem. Phys.* **2007**, *127*, 234101.
(38) Hazra, A.; Nooijen, M. Vibronic coupling in the excited cationic states of ethylene: Simulation of the photoelectron spectrum between 12 and 18 eV. *J. Chem. Phys.* **2005**, *122*, 204327.
(39) Tang, J.; Lee, M. T.; Lin, S. H. Effects of the Duschinsky mode-mixing mechanism on temperature dependence of electron transfer processes. *J. Chem. Phys.* **2003**, *119*, 7188−7196.
(40) Borrelli, R.; Peluso, A. The temperature dependence of radiationless transition rates from ab initio computations. *Phys. Chem. Chem. Phys.* **2011**, *13*, 4420−4426.
(41) Wilson, E. B.; Decius, J. C.; Cross, P. C. *Molecular Vibrations. The Theory of Infrared and Raman Vibrational Spectra*; Dover, 1955; pp 54−76.
(42) Pulay, P.; Fogarasi, G. Geometry optimization in redundant internal coordinates. *J. Chem. Phys.* **1992**, *96*, 2856−2860.
(43) Peng, C.; Ayala, P. Y.; Schlegel, H. B.; Frisch, M. J. Using redundant internal coordinates to optimize equilibrium geometries and transition states. *J. Comput. Chem.* **1996**, *17*, 49−56.
(44) Califano, S. *Vibrational States*; J. Wiley and Sons, Ltd.: London, 1976.
(45) Santoro, F.; Improta, R.; Lami, A.; Bloino, J.; Barone, V. Effective method to compute Franck−Condon integrals for optical spectra of large molecules in solution. *J. Chem. Phys.* **2007**, *126*, 084509.
(46) Ozkan, I. Franck−Condon principle for polyatomic molecules: Axis-switching effects and transformation of normal coordinates. *J. Mol. Spectrosc.* **1990**, *139*, 147−162.
(47) Sando, G. M.; Spears, K. G. Ab initio computation of the Duschinsky mixing of vibrations and nonlinear effects. *J. Phys. Chem. A* **2001**, *105*, 5326−5333.
(48) Requena, A.; Cerón-Carrasco, J. P.; Bastida, A.; Zúñiga, J.; Miguel, B. A density functional theory study of the structure and vibrational spectra of β-carotene, capsanthin, and capsorubin. *J. Phys. Chem. A* **2008**, *112*, 4815−4825.
(49) Guo, W.-H.; Tu, C.-Y.; Hu, C.-H. *Cis*−*trans* isomerizations of β-carotene and lycopene: A theoretical study. *J. Phys. Chem. B* **2008**, *112*, 12158−12167.
(50) Cerón-Carrasco, J. P.; Bastida, A.; Zúñiga, J.; Requena, A.; Miguel, B. Density functional theory study of the stability and vibrational spectra of the β-carotene isomers. *J. Phys. Chem. A* **2009**, *113*, 9899−9907.
(51) Durbeej, B.; Eriksson, L. A. Protein-bound chromophores astaxanthin and phytochromobilin: Excited state quantum chemical studies. *Phys. Chem. Chem. Phys.* **2006**, *8*, 4053−4071.
(52) Martins, J. a. B. L.; Durães, J. A.; Sales, M. J. A.; Vilela, A. F. A.; e Silva, G. M.; Gargano, R. Theoretical investigation of carotenoid ultraviolet spectra. *Int. J. Quantum Chem.* **2009**, *109*, 739−745.
(53) García, G.; Ciofini, I.; Fernández-Gómez, M.; Adamo, C. Confinement effects on UV−visible absorption spectra: β-carotene inside carbon nanotube as a test case. *J. Phys. Chem. Lett.* **2013**, *4*, 1239−1243.
(54) Larsen, D. S.; Papagiannakis, E.; van Stokkum, I. H.; Vengris, M.; Kennis, J. T.; van Grondelle, R. Excited state dynamics of β-carotene explored with dispersed multi-pulse transient absorption. *Chem. Phys. Lett.* **2003**, *381*, 733−742.
(55) Frank, H. A.; Bautista, J. A.; Josue, J. S.; Young, A. J. Mechanism of nonphotochemical quenching in green plants: Energies of the

lowest excited singlet states of violaxanthin and zeaxanthin. *Biochemistry* **2000**, *39*, 2831−2837.
(56) Tatchen, J.; Pollak, E. Ab initio spectroscopy and photoinduced cooling of the *trans*-stilbene molecule. *J. Chem. Phys.* **2008**, *128*, 164303.
(57) Peng, Q.; Niu, Y.; Deng, C.; Shuai, Z. Vibration correlation function formalism of radiative and non-radiative rates for complex molecules. *Chem. Phys.* **2010**, *370*, 215−222.
(58) Borrelli, R.; Capobianco, A.; Peluso, A. Generating function approach to the calculation of spectral band shapes of free-base chlorin including Duschinsky and Herzberg−Teller effects. *J. Phys. Chem. A* **2012**, *116*, 9934−9940.
(59) Baiardi, A.; Bloino, J.; Barone, V. General time dependent approach to vibronic spectroscopy including Franck−Condon, Herzberg−Teller, and Duschinsky effects. *J. Chem. Theory Comput.* **2013**, *9*, 4097−4115.
(60) Kubo, R.; Toyozawa, Y. Application of the method of generating function to radiative and non-radiative transitions of a trapped electron in a crystal. *Prog. Theor. Phys.* **1955**, *13*, 160−182.
(61) Mukamel, S.; Abe, S.; Islampour, R. Generating function for electronic spectra of polyatomic molecules. *J. Phys. Chem.* **1985**, *89*, 201−204.
(62) Santoro, F.; Lami, A.; Improta, R.; Bloino, J.; Barone, V. Effective method for the computation of optical spectra of large molecules at finite temperature including the Duschinsky and Herzberg−Teller effect: The Qx band of porphyrin as a case study. *J. Chem. Phys.* **2008**, *128*, 224311.
(63) Barone, V.; Bloino, J.; Biczysko, M.; Santoro, F. Fully integrated approach to compute vibrationally resolved optical spectra: From small molecules to macrosystems. *J. Chem. Theory Comput.* **2009**, *5*, 540−554.
(64) Bloino, J.; Biczysko, M.; Santoro, F.; Barone, V. General approach to compute vibrationally resolved one-photon electronic spectra. *J. Chem. Theory Comput.* **2010**, *6*, 1256−1274.
(65) (a) Santoro, F. *FCclasses, a Fortran 77 code*, http://village.pi.iccom.cnr.it (accessed July 1, 2013); (b) Cerezo, J.; Santoro, F. *TDspectrum, a routine for TD calculations within FCclasses*.
(66) Frisch, M. J.; Trucks, G. W.; Schlegel, H. B.; Scuseria, G. E.; Robb, M. A.; Cheeseman, J. R.; Scalmani, G.; Barone, V.; Mennucci, B.; Petersson, G. A.; Nakatsuji, H.; Caricato, M.; Li, X.; Hratchian, H. P.; Izmaylov, A. F.; Bloino, J.; Zheng, G.; Sonnenberg, J. L.; Hada, M.; Ehara, M.; Toyota, K.; Fukuda, R.; Hasegawa, J.; Ishida, M.; Nakajima, T.; Honda, Y.; Kitao, O.; Nakai, H.; Vreven, T.; Montgomery, J. A.; Jr., Peralta, J. E.; Ogliaro, F.; Bearpark, M.; Heyd, J. J.; Brothers, E.; Kudin, K. N.; Staroverov, V. N.; Kobayashi, R.; Normand, J.; Raghavachari, K.; Rendell, A.; Burant, J. C.; Iyengar, S. S.; Tomasi, J.; Cossi, M.; Rega, N.; Millam, J. M.; Klene, M.; Knox, J. E.; Cross, J. B.; Bakken, V.; Adamo, C.; Jaramillo, J.; Gomperts, R.; Stratmann, R. E.; Yazyev, O.; Austin, A. J.; Cammi, R.; Pomelli, C.; Ochterski, J. W.; Martin, R. L.; Morokuma, K.; Zakrzewski, V. G.; Voth, G. A.; Salvador, P.; Dannenberg, J. J.; Dapprich, S.; Daniels, A. D.; Farkas, O.; Foresman, J. B.; Ortiz, J. V.; Cioslowski, J.; and Fox, D. J. *Gaussian 09*, Revision A.2; Gaussian Inc.: Wallingford, CT, 2009.
(67) Sibert, E. L.; Hynes, J. T.; Reinhardt, W. P. Fermi resonance from a curvilinear perspective. *J. Phys. Chem.* **1983**, *87*, 2032−2037.
(68) Stendardo, E.; Avila Ferrer, F.; Santoro, F.; Improta, R. Vibrationally resolved absorption and emission spectra of dithiophene in the gas phase and in solution by first-principle quantum mechanical calculations. *J. Chem. Theory Comput.* **2012**, *8*, 4483−4493.
(69) Avila Ferrer, F. J.; Cerezo, J.; Stendardo, E.; Improta, R.; Santoro, F. Insights for an accurate comparison of computational data to experimental absorption and emission spectra: Beyond the vertical transition approximation. *J. Chem. Theory Comput.* **2013**, *9*, 2072−2082.